Measurement of the contribution of neutrons to hadron calorimeter signals

N. Akchurin[a], L. Berntzon[a], A. Cardini[b], R. Ferrari[c], G. Gaudio[c], J. Hauptman[d], H. Kim[a], L. La Rotonda[e], M. Livan[c], E. Meoni[e], H. Paar[f], A. Penzo[g], D. Pinci[h], A. Policicchio[e], S. Popescu[i,1], G. Susinno[e], Y. Roh[a], W. Vandelli[c], R. Wigmans[a,*]

[a]*Texas Tech University, Lubbock (TX), USA*
[b]*Dipartimento di Fisica, Università di Cagliari and INFN Sezione di Cagliari, Italy*
[c]*Dipartimento di Fisica Nucleare e Teorica, Università di Pavia and INFN Sezione di Pavia, Italy*
[d]*Iowa State University, Ames (IA), USA*
[e]*Dipartimento di Fisica, Universitá della Calabria and INFN Cosenza, Italy*
[f]*University of California at San Diego, La Jolla (CA), USA*
[g]*INFN Trieste, Italy*
[h]*Dipartimento di Fisica, Università di Roma "La Sapienza" and INFN Sezione di Roma, Italy*
[i]*CERN, Genève, Switzerland*

Abstract

The contributions of neutrons to hadronic signals from the DREAM calorimeter are measured by analyzing the time structure of these signals. The neutrons, which mainly originate from the evaporation stage of nuclear breakup in the hadronic shower development process, contribute through elastic scattering off protons in the plastic scintillating fibers which provide the dE/dx information in this calorimeter. This contribution is characterized by an exponential tail in the pulse shape, with a time constant of $\sim 25\,\mathrm{ns}$. The relative contribution of neutrons to the signals increases with the distance from the shower axis. As expected, the neutrons do not contribute to the DREAM Cherenkov signals.
© 2007 Elsevier B.V. All rights reserved.

1. Introduction

The energy resolution of calorimeters is determined by fluctuations. To improve the resolution of a given calorimeter significantly, one has to address the dominating source of these fluctuations. In non-compensating calorimeters, fluctuations in the electromagnetic shower fraction (f_{em}) dominate the energy resolution for hadrons and jets. These fluctuations, and their energy-dependent characteristics, are also responsible for other undesirable calorimeter characteristics, in particular hadronic signal non-linearity and a non-Gaussian response function.

The DREAM (Dual-REAdout Method) calorimeter was developed as a device that would make it possible to eliminate the effects of these fluctuations. The detector is based on a copper absorber structure, equipped with two types of active media which measure complementary characteristics of the shower development. Scintillating fibers measure the total energy deposited by the shower particles, while Cherenkov light is only produced by the charged, relativistic shower particles. Since the latter are almost exclusively found in the electromagnetic (em)

*Corresponding author. Fax: +1 806 742 1182.
  E-mail address: wigmans@ttu.edu (R. Wigmans).
  [1]On leave from IFIN-HH, Bucharest, Romania.

shower component (dominated by π^0s produced in hadronic showers), a comparison of the two signals makes it possible to measure f_{em}, event by event. As a result, the effects of fluctuations in this component can, for all practical purposes, be eliminated. This leads to an important improvement in the hadronic calorimeter performance. The performance characteristics of this detector are described elsewhere [1–3].

The elimination of (the effects of) the dominant source of fluctuations means that other types of fluctuations now dominate the detector performance. Further improvements may be obtained by concentrating on these. The energy resolution of a calorimeter of the type described above is limited by fluctuations in the Cherenkov light yield and by sampling fluctuations. In another paper, we demonstrate that these effects may be effectively reduced by using a homogeneous calorimeter that produces a (separable) mixture of scintillation and Cherenkov light [4].

Once the mentioned effects have been eliminated, the performance of this type of detector may approach the theoretical hadronic energy resolution limit. This limit is determined by the so-called fluctuations in *visible energy*, which result from the fact that some (variable) fraction of the energy carried by the showering particle is used to provide the nuclear binding energy needed to release nucleons and nucleon aggregates in nuclear reactions. This energy does itself not result in a measurable signal. However, it has been shown that efficient detection of the neutrons abundantly produced in these processes may be an effective tool for reducing the (effects of) fluctuations in visible energy, and that hadronic energy resolutions of $15-20\%/\sqrt{E}$ might be achieved this way [5]. In the present paper, we report on efforts to measure the contribution of neutrons to the signals of the DREAM calorimeter.

In Section 2, we briefly discuss the reasons for the importance of neutrons in this context, and we describe the experimental technique we used to get a handle on their contributions to the calorimeter signals. In Section 3, we describe the calorimeter and the experimental setup in which it was tested. Experimental results are presented, discussed and compared with results from other experiments in Section 4. Summarizing conclusions are given in Section 5.

2. Neutrons in hadron calorimetry

2.1. The role of neutrons

When an incoming high-energy hadron strikes an atomic nucleus, the most likely process to occur is spallation. Spallation is usually described as a two-stage process: a fast intranuclear cascade, followed by a slower evaporation stage. The incoming hadron makes quasi-free collisions with nucleons inside the struck nucleus. The affected nucleons start traveling themselves through the nucleus and collide with other nucleons. In this way, a cascade of fast nucleons develops. In this stage, also pions and other

unstable hadrons may be created if the transferred energy is sufficiently high. Some of the particles taking part in this cascade reach the nuclear boundary and escape. Others get absorbed and distribute their kinetic energy among the remaining nucleons in the nucleus, resulting in the production of an excited intermediate nucleus.

The second step of the spallation reaction consists of the de-excitation of this intermediate nucleus. This is achieved by evaporating a certain number of particles, predominantly free nucleons, but sometimes also α's or even heavier nucleon aggregates, until the excitation energy is less than the binding energy of a single nucleon. The remaining energy, typically a few MeV, is released in the form of γ rays. In very heavy nuclei, e.g., uranium, the intermediate nucleus may also fission.

In these spallation reactions, considerable numbers of nucleons may be released from the nuclei in which they are bound. The energy needed to release these nucleons, i.e., the nuclear binding energy, is lost for calorimetric purposes. It does not contribute to the calorimeter signal, and is thus called "*invisible*".

There is a large variety of processes that may occur in hadronic shower development and event-to-event fluctuations in the invisible energy fraction are substantial. On average, invisible energy accounts for 30–40% of the non-em shower energy, i.e., energy that is not carried by π^0s or other electromagnetically decaying particles produced in the shower development [6–8].

The large event-to-event fluctuations in visible energy have obviously direct consequences for the precision with which hadronic energy can be measured in calorimeters. Because of these fluctuations, which have no equivalent in electromagnetic shower development processes, the energy resolution with which hadron showers can be measured is usually considerably worse than the resolution with which em showers can be measured. There is, however, an elegant way in which one can limit these effects, by exploiting the correlation that exists between the invisible energy lost in releasing nucleons from the nuclei in which they are bound and the kinetic energy carried by these nucleons [9,10].

As indicated above, the nucleons produced in spallation reactions can be divided into two classes, the *cascade* and the *evaporation* nucleons. The energy spectrum of the latter is considerably softer and most of these nucleons are neutrons. This is because the Coulomb barrier prevents soft protons from being released and also because of the larger abundance of neutrons in target nuclei. The evaporation neutrons carry an average kinetic energy of 2–3 MeV. The cascade nucleons are more energetic, but also much less numerous than the evaporation nucleons. Therefore, the vast majority of the nucleons released in hadronic shower development are *neutrons*, especially in high-Z materials.

Experimental measurements have revealed that the numbers of neutrons produced in hadronic shower development are large, e.g., 20 per GeV in lead absorber [11]. There is a clear correlation between the total amount of

invisible energy (i.e., the number of target nucleons released in the development of the hadron shower) and the total kinetic energy carried by these neutrons. This correlation can be exploited to achieve a substantial improvement of the calorimetric performance [7,9,10].

2.2. How to detect shower neutrons?

Shower neutrons can only be detected through the effects of the nuclear reactions they initiate. The most abundant nuclear evaporation neutrons are produced with typical kinetic energies of a few MeV. At these energies, the most important process through which they lose this kinetic energy is *elastic scattering*. After they have lost practically all their kinetic energy, the neutrons may be captured by a nucleus, and generate typically 7–8 MeV in the form of nuclear γs, when this compound nucleus falls back to its ground state. However, since the thermalization process that precedes this capture takes typically of the order of 1 μs [12], the latter process is in practice not helpful for improving calorimetric performance. This may be concluded from studies by members of the ZEUS Collaboration [13,14], who measured the hadronic energy resolution and e/π signal ratios for their ^{238}U/plastic-scintillator calorimeter as a function of the signal integration time. The contributions from neutron capture were clearly observed in these studies, but benefits to the energy resolution were offset by increased noise contributions at long signal integration times.

Since the average energy fraction transferred in elastic scattering scales with $(A + 1)^{-1}$, hydrogenous materials are the most efficient neutron moderators. In sampling calorimeters with hydrogenous active material, the recoil protons may contribute to the calorimeter signals. Acosta et al. [15] have demonstrated that the average time between subsequent elastic scattering processes in that case is approximately constant, and since the energy fraction transferred to the protons is, on average, constant as well (50%), this contribution manifests itself as an exponential tail to the time structure of the signals. This is the signature we have looked for in the present study.

In Ref. [15], the time constant of the exponential tail was measured to be 9.9 ns. The time constant in the detector used for our studies may be estimated as follows. Hydrogen atoms were contained in the plastic fibers that yielded the signals in this detector. These fibers constituted 17.4% of the total detector volume, which further contained copper (69.3%), silicon (4.6%) and air (8.7%). Assuming that plastic contains equal numbers of hydrogen and carbon atoms, and has a density of 1 g/cm³, we calculated a density of 8×10^{21} hydrogen atoms per cm³.

The cross-section for elastic neutron–proton scattering in the relevant energy range increases from 2.2 b at 3 MeV to 12 b at 0.1 eV [16]. Therefore, the average distance traveled by neutrons between subsequent np scattering processes varied from 56 cm at 3 MeV to 10 cm at 0.1 MeV, while the velocity of the neutrons decreased from 0.08c at 3 MeV to 0.015c at 0.1 MeV. As a result, the *time* between subsequent np scatters was the same for these two energies: 23 ns. This is of course the reason for the exponentially decreasing contribution of the neutrons to the signal. In each np scatter, the neutrons lose, on average, the same fraction of their energy: 50%. If no other energy loss mechanisms than elastic np scattering would play a role, the kinetic energy of the neutrons would thus decrease by a factor e in 33 ns. Other, competing energy loss processes would speed up this decrease. Such processes include elastic scattering off C, Si and Cu nuclei, as well as inelastic $(n, n'\gamma)$ scattering, mainly off ^{63,65}Cu nuclei (lowest excited states ∼0.7 MeV). We estimate these processes to decrease the time constant of the neutron tail to ∼25 ns.

As indicated above, the mean free path of the evaporation neutrons is quite large. Neutrons produced at 3 MeV travel on average half a meter before undergoing their first scatter off a free proton. This means that the radial profile of the neutron contribution to the signals is much broader than that of the other shower particles, whose profile is governed by the Molière radius (for the em shower component) and the nuclear interaction length. Therefore, the relative contribution of neutrons to the scintillation signals should increase with the radial distance to the shower axis. Since the recoil protons are non-relativistic, they do not generate Cherenkov light. In summary, the signature we are looking for thus has the following characteristics:

- An exponential tail in the time structure of the signals, with a time constant of ∼25 ns.
- The relative importance of this tail, i.e., of its contribution to the total calorimeter signal, should increase with the distance to the shower axis.
- The tail should be absent in the time structure of calorimeter signals based on Cherenkov light.

In the following, we describe our search for an experimental signature of this type.

3. Experimental details

3.1. The detector

The detector used for our studies was the DREAM calorimeter, which has been described in considerable detail elsewhere [1–3]. The basic element of this detector (see Fig. 1) is an extruded copper rod, 2 m long and 4×4 mm² in cross-section. This rod is hollow, and the central cylinder has a diameter of 2.5 mm. Seven optical fibers are inserted in this hole. Three of these are plastic scintillating fibers,[2] the other four fibers are undoped[3] and are intended for detecting Cherenkov light.
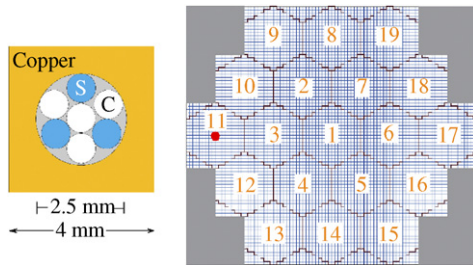

Fig. 1. The basic building block of the DREAM calorimeter is a $4 \times 4\,mm^2$ extruded hollow copper rod of 2 m length, with a 2.5 mm diameter central hole. Seven optical fibers (four undoped and three scintillating fibers) with a diameter of 0.8 mm each are inserted in this hole, as shown in the left diagram. The right diagram shows a cross-section of the calorimeter, which consists of 19 hexagonal towers. The impact point of the beam (center of Tower #11) is indicated as well.

The DREAM detector consisted of 5580 such rods, 5130 of these were equipped with fibers. The empty rods were used as fillers, on the periphery of the detector. The instrumented volume thus had a length of 2.0 m, an effective radius of 16.2 cm, and a mass of 1030 kg. The calorimeter's radiation length (X_0) was 20.1 mm, its Moliére radius (ρ_M) 20.4 mm and its nuclear interaction length (λ_{int}) 200 mm.

The fibers were grouped to form 19 readout towers. Each tower consisted of 270 rods and had an approximately hexagonal shape (80 mm apex to apex). The effective radius of each tower was 37.1 mm $(1.82\rho_M)$. A central tower (#1) was surrounded by two hexagonal rings, the Inner Ring (six towers, numbered 2–7) and the Outer Ring (12 towers, numbered 8–19). The towers were not segmented in the longitudinal direction.

The fibers leaving the rear of this structure were separated into bunches: one bunch of scintillating fibers and one bunch of Cherenkov fibers for each tower, 38 bunches in total. In this way, the readout structure was established (see Fig. 1). Each bunch was coupled through a 2 mm air gap to a photomultiplier tube (PMT).[4] Much more information about this calorimeter is provided in Refs. [1–3].

3.2. The beam line

The measurements described in this paper were performed in the H4 beam line of the Super Proton Synchrotron at CERN. The DREAM detector was mounted on a platform that could move vertically and sideways with respect to the beam. For the measurements described here, we only used one detector position, namely where the beam entered the detector parallel to its axis (the "0°" orientation), in the center of Tower #11.

Two small scintillation counters provided the signals that were used to trigger the data acquisition system. These Trigger Counters were 2.5 mm thick, and the area of

overlap was $6 \times 6\,cm^2$. A coincidence between the logic signals from these counters provided the trigger.

3.3. Data acquisition

Measurement of the time structure of the calorimeter signals formed a crucial part of the tests described here. In order to limit distortion of this structure as much as possible, we used 15 mm thick air-core cables to transport four selected calorimeter signals to the counting room. Such cables were also used for the trigger signals, and these were routed such as to minimize delays in the DAQ system.[5]

The other calorimeter signals were transported through RG-58 cables with (for timing purposes) appropriate lengths to the counting room. The signals used for the neutron measurements were split (passively) into three equal parts in the counting room. One part was sent to a charge ADC, the other two signals were used for analysis of the time structure by means of a FADC. The latter unit measured the amplitude of the signals at a rate of 200 MHz. During a time interval of 80 ns, 16 measurements of the amplitude were thus obtained. The two signals from the splitter box were measured separately in two different channels of the FADC module.[6] The second signal was delayed by 2.5 ns with respect to the first one. By using two channels of the FADC module for each calorimeter signal, the time structure of the signals was thus effectively measured with a resolution of 2.5 ns (400 MHz).

The charge measurements were performed with 12-bit LeCroy 1182 ADCs. These had a sensitivity of 50 fC/count and a conversion time of 16 μs. The ADC gate width was 100 ns, and the calorimeter signals arrived ∼20 ns after the start of the gate. The data acquisition system used VME electronics. The chosen scheme optimized the CPU utilization and increased the data taking efficiency by exploiting the bunch structure of the SPS, where beam particles were provided to our experiment during a spill of 4.8 s, out of a total cycle time of 16.8 s. It allowed a data acquisition rate as high as 2 kHz, limited by the FADC readout time. The typical event size was ∼1 kB.

3.4. Calibration of the detectors

Using the high voltage, the gain in all PMTs was set to generate ∼1 pC/GeV. The 38 PMTs reading out the 19 towers were calibrated with 50 GeV electrons. The showers generated by these particles were not completely contained in a single calorimeter tower. The (average) containment was found from EGS4 Monte Carlo simulations. When the electrons entered a tower in its geometrical center, on average 92.5% of the scintillation light and 93.6% of the Cherenkov light was generated in that tower [1]. The remaining fraction of the light was shared by the

---

[4]Hamamatsu R-580, a 10-stage, 1.5 in. PMT with a nominal gain of 3.7×10^5 at 1250 V.

[5]We measured the signal speed to be 0.78c in these cables.
[6]Dr. Struck SIS3320, http://www.struck.de/sis3320.htm.

surrounding towers. The signals observed in the exposed tower thus corresponded to an energy deposit of 46.3 GeV in the case of the scintillating fibers and of 46.8 GeV for the Cherenkov fibers. This, together with the precisely measured values of the average signals from the exposed tower, formed the basis for determining the calibration constants, i.e., the relationship between the measured number of ADC counts and the corresponding energy deposit.

3.5. Experimental data

The experiments were carried out with a beam of 100 GeV π^+ which was steered into the center of Tower #11. In all measurements, the scintillation and Cherenkov signals from this (on-axis) tower were sent through the air-core cables for time structure analysis, using $2 \times 2 = 4$ channels of the FADC unit. The other four FADC channels were used to measure the time structure of the signals from an off-axis tower. In separate runs, we used the signals from Tower #3 (located at an average radial distance of 72 mm from the beam axis), Tower #1 (radial distance 144 mm) and Tower #6 (radial distance 216 mm) for that purpose. In each run, 100 000 events were collected.

4. Experimental results

4.1. Time structure of the DREAM signals

The FADC measurements provided considerable detail on the time structure of the signals generated by the calorimeter. This is illustrated in Fig. 2, which shows the average time structure of the scintillator and Cherenkov
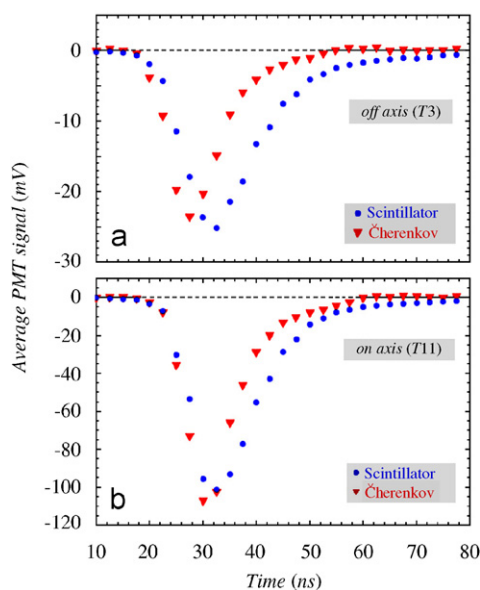
signals measured in the neighboring Towers #11 (on-axis) and #3 (off-axis), with a sampling frequency of 400 MHz (2.5 ns time samples). Two general features should be pointed out:

- The starting point of the pulse is not the same for all four signals, as a result of differences in cable lengths and PMT transit times. In particular, the signals from Tower #3 started about 2.5 ns earlier than those from Tower #11.
- The input impedances of the channels that recorded the signals from the off-axis tower were four times smaller than those of the channels that handled the signals from the on-axis tower. Therefore, the vertical scale of the bottom plot should be multiplied by a factor of 4 in order to be compatible with the top one.

The figure also shows that the Cherenkov signals are considerably faster than the scintillation ones. This should of course be expected, since the scintillation process is characterized by one or several time constants, while Cherenkov light emission is prompt. For our purpose it is also interesting to compare the corresponding signals from the two different calorimeter towers with each other. This is because the relative contribution of neutrons to the signals increases with the distance to the shower axis.

Fig. 3 shows the time structure of the Cherenkov signals from Towers #11 and #3 in one plot. The time axis of the Tower #3 signal has been shifted by 2.5 ns to make the starting points of both signals the same. In order to be able to compare the pulse shapes, we have normalized both signals on the basis of their integrated pulse shape. The result shows no significant differences between the time structures of the Cherenkov signals from these two towers. Since the low-energy neutrons do not contribute to the Cherenkov signals from this calorimeter other than through capture γs (which fall outside the 80 ns time scale considered here), we did not expect to see a difference.

The situation is quite different for the scintillation signals. Fig. 4 shows the average time structure of the
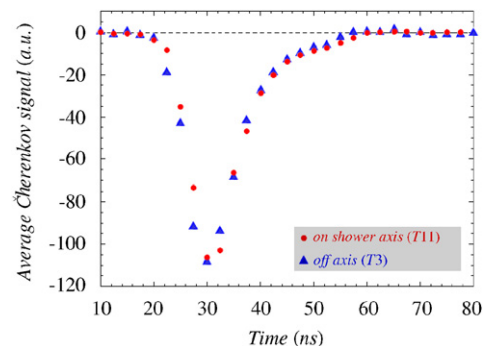

Fig. 2. Average time structure of the scintillator and Cherenkov signals measured for 100 GeV π^+ showers in a DREAM tower (#11) located on the shower axis (b) and in a tower (#3) located at a distance of 72 mm off-axis (a).

Fig. 3. Comparison of the average time structure of the Cherenkov signals measured for 100 GeV π^+ showers in a DREAM tower (#11) located on the shower axis and in a tower (#3) located at a distance of 72 mm off-axis. The signals have been normalized such that the integral over the pulse shape is the same in both cases.

scintillation signals from Towers #11 and #3 in a logarithmic display. As in Fig. 3, the integrated pulse shapes have been equalized in order to facilitate a comparison between these time structures. The figure shows that the trailing edge of the signal from Tower #11 is, on average, clearly steeper than that of the Tower #3 pulse. Since an eventual contribution of neutrons to the scintillator signals is expected to increase with the distance to the shower axis, this is precisely the effect one would expect to see.

Fig. 5 shows a comparison between the average Cherenkov and scintillator signals from Tower #11. The signals have been inverted and are logarithmically displayed, so that differences in the signal shapes are emphasized. The trailing edge of the Cherenkov pulse shape is well described by a single exponential function,
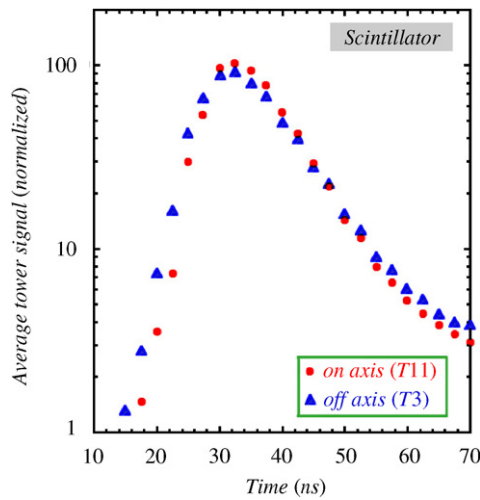
with a time constant of ~7 ns. Such a function also describes the initial portion of the trailing edge of the scintillator pulse shape. However, the latter shape exhibits clearly an additional, slower component. The curve drawn in Fig. 5b corresponds to a time constant of 20 ns for this slow component.

We fitted the trailing edge of the average scintillator signal distributions observed in Towers #11, 3, 1 and 6 to an expression of the following type:

$$N(t) = N_1 e^{-t/\tau_1} + N_2 e^{-t/\tau_2} \qquad (1)$$

where the decay time constants τ_1 and τ_2 were kept at fixed values, and the signal values N_1 and N_2 were optimized in the fit. The ratio N_2/N_1 is a measure for the relative contribution of neutrons to the scintillator signals. The precise value of this contribution was found by calculating

$$f_n = \frac{\int_{t_0}^{\infty} N_2 e^{-t/\tau_2} \, dt}{\int_{t_0}^{\infty} (N_1 e^{-t/\tau_1} + N_2 e^{-t/\tau_2}) \, dt} \qquad (2)$$

where t_0 is chosen such that

$$\int_{t_0}^{\infty} (N_1 e^{-t/\tau_1} + N_2 e^{-t/\tau_2}) \, dt = \Sigma_i S_i \qquad (3)$$

the experimentally measured integrated pulse shape, shown in Fig. 5b. The value of τ_1 was kept constant at 7 ns throughout these studies, whereas for τ_2 values of 20, 25 and 33 ns were used. Because of the limited time interval over which the time structure was measured, and the relatively small contribution of the slow component to the total signals, it was not possible to measure τ_2 with very high precision, although the value of 25 ns estimated in our analysis described in Section 2.2 is most definitely not far off the mark. Yet, the results of this analysis show clearly that the relative contribution of neutrons to the total scintillator signals (f_n) increases with the distance from the shower axis. This is illustrated in Fig. 6, where f_n is shown
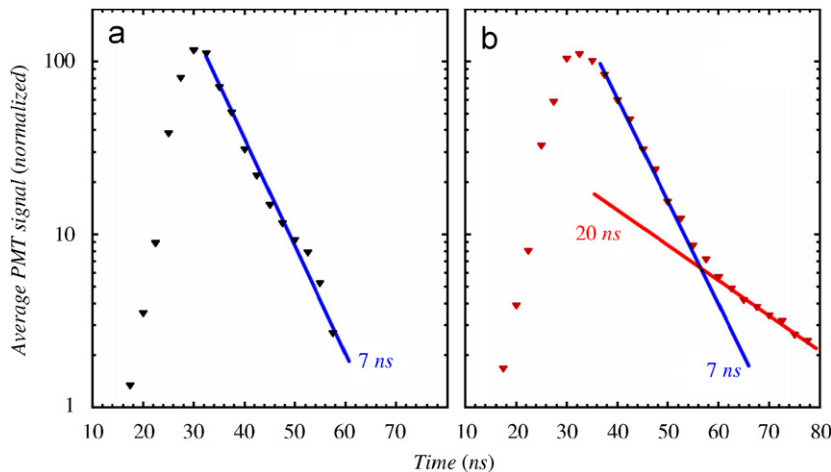

Fig. 4. Comparison of the average time structure of the scintillator signals measured for 100 GeV π^+ showers in a DREAM tower (#11) located on the shower axis and in a tower (#3) located at a distance of 72 mm off-axis. The measured signals have been inverted.

Fig. 5. The average time structure of the Cherenkov (a) and scintillator (b) signals measured for 100 GeV π^+ showers in DREAM Tower #11, located on the shower axis. The measured signals have been inverted. The lines represent exponential fits to (parts of) the trailing edge of the signal shapes.
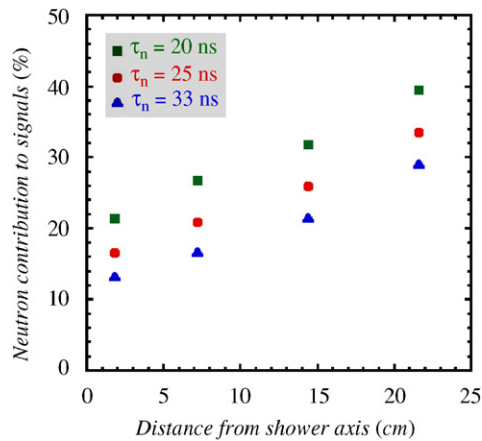
Fig. 6. The average percentage of the scintillation signals from 100 GeV π^+ showers attributed to elastic neutron–proton scattering in the plastic fibers, for four different DREAM towers, located at different, increasing distances from the shower axis. Results are given for three different choices of the time constant assumed for this neutron contribution. See text for details.

for Towers #11, 3, 1 and 6. For each of the three mentioned values of the decay time constant τ_2, the average neutron contribution approximately doubles, from ~15% to ~30%, when going out from the shower axis (the center of Tower #11) to Tower #6, whose center is located at 21.6 cm from the shower axis.

4.2. Comparison with other experiments

Fundamental understanding of hadron calorimetry has greatly benefited from a variety of efforts by the ZEUS Collaboration. Members of this Collaboration have also performed a number of systematic studies of the time structure of hadronic calorimeter signals [13,14]. These measurements extended over a considerably longer gate width (up to 4 μs) than in our case, mainly because they wanted to investigate if and to what extent the predicted contributions from thermal neutron capture in their uranium-based calorimeters [12] would affect the response function. The measurements were also carried out with a considerably smaller sampling frequency (60 MHz [14], vs. 400 MHz in the present study).

The time structure of the ZEUS signals exhibited three different time constants, when fitted to a sum of exponentials [14]. The values of these time constants were approximately 10, 100 and 1000 ns. In total, these three delayed components contributed 40–50% to the total hadronic signals. The contribution of the remaining, prompt component increased with energy, consistent with the trend observed for the em shower fraction (f_{em}). Most of the delayed signal fraction (>80%) was contained in the fastest component. We believe that this component (for which the authors report a time constant of 9 ns) has the same origin as the exponential tail observed in the present study, and the 10 ns component measured by

SPACAL [15]. The slowest (1 μs) component observed in the ZEUS study is consistent with thermal neutron capture. Because of the short time interval over which signals were sampled in the present study, our measurements are completely insensitive to eventual contributions of small, slow components as observed by ZEUS.

Even though a detailed comparison between the ZEUS and DREAM results is complicated by a number of important differences, it is interesting to note that ZEUS did observe a similar dependence of the relative contribution of delayed signal components on the distance from the shower axis. Ref. [14] reports results from signals observed in rings consisting of detector cells located at approximately equal distance from the shower axis. When the integration time was increased from 100 ns to 3 μs, the fractional increase in the signals from four rings with increasing radii was measured to be 11%, 19%, 34% and 44%, respectively. This is the same trend as we observed in Fig. 6 and an important argument in support of neutrons being responsible for the observed effects.

5. Conclusions

We have analyzed the time structure of hadronic signals from the DREAM calorimeter, with a sampling frequency of 400 MHz (2.5 ns time bins), for towers located at different distances from the shower axis. We have found a clear indication for the contribution of evaporation neutrons to the scintillation signals from this detector. These neutrons contribute through elastic scattering of protons in the plastic scintillating fibers which provide the dE/dx information in this calorimeter. Their contribution can be described by an exponential tail in the pulse shape, with a time constant of ~25 ns. The contribution of neutrons to the signals increases with the distance from the shower axis, and represents up to ~30% of the total signal from off-axis towers. As expected, the neutrons do not contribute at all to the DREAM Cherenkov signals.

References

[1] N. Akchurin, et al., Nucl. Instr. and Meth. A 536 (2005) 29.
[2] N. Akchurin, et al., Nucl. Instr. and Meth. A 537 (2005) 537.
[3] N. Akchurin, et al., Nucl. Instr. and Meth. A 533 (2004) 305.
[4] N. Akchurin, et al., Nucl. Instr. and Meth. (2007), submitted for publication, preprint arXiv:0707.4021[physics.ins-det].
[5] R. Wigmans, Calorimetry—Energy Measurement in Particle Physics, International Series of Monographs on Physics, vol. 107, Oxford University Press, Oxford, 2000.
[6] T.A. Gabriel, et al., Nucl. Instr. and Meth. A 338 (1994) 336.

[7] R. Wigmans, Rev. Sci. Instr. 69 (1998) 3723 and references therein.

[8] D.E. Groom, Nucl. Instr. and Meth. 572 (2007) 633.

[9] E. Bernardi, et al., Nucl. Instr. and Meth. A 262 (1987) 229.

[10] D. Acosta, et al., Nucl. Instr. and Meth. A 316 (1992) 184.

[11] C. Leroy, Y. Sirois, R. Wigmans, Nucl. Instr. and Meth. A 252 (1986) 4–28.

[12] H. Brückmann, et al., Nucl. Instr. and Meth. A 263 (1988) 136.

[13] J. Krüger, The uranium/scintillator calorimeter for the ZEUS detector at the electron–proton collider HERA, Internal Report DESY F35-92-02, DESY Hamburg, 1992.

[14] A. Caldwell, et al., Nucl. Instr. and Meth. A 330 (1993) 389.

[15] D. Acosta, et al., Nucl. Instr. and Meth. A 302 (1991) 36.

[16] L. Stewart, Hydrogen scattering cross section, ^1H (n,n) ^1H, Los Alamos Report LA-7899-MS, 1979.